

Light Scattering of Silver Halide Crystals

H. Dahl¹, H. J. Metz², T. Wriedt³

¹Universität Bremen, Badgasteiner Str. 3, D-28359 Bremen

²Agfa-Gaevert AG, Kaiser-Wilhelm-Allee, D-51373 Leverkusen

³Institut für Werkstofftechnik, Badgasteiner Str. 3, D-28234 Bremen

Abstract

The light scattering process of plane waves by silver halide crystals plays an important role in development and optimization of silver halide photographic films. Mie theory is used for scattering calculations of such crystals because the influence of the crystal geometry is neglectable with the normal cubic shape. Since scattering of crystals can be calculated by other theories which are not restricted to spherical shapes, theoretical optimization of such films by crystal shape becomes possible. In this paper the Multiple Multipole Method is used for simulating scattering by oblate silver halide crystals.

1 Introduction

Progress in silver halide photography can be achieved by increasing the sensitivity of a photographic film without any decrease of its resolution. Therefore, the elastic scattering process of the incident light with the silver halide crystals within the photosensitive film becomes more and more interesting. For example, the calculated scattering distributions of single crystals can be used for Monte-Carlo simulation to compute the modulation transfer function of a photographic film [1].

Because of the large relative refractive index of about 1.5 between the silver halide crystals and the embedding gelatine matrix, the crystals with diameters of about 1 μm have to be taken as Mie scatterers with a large relative scattering cross section. For this reason, the crystals itself cause a diffusion of the parallel incident photons and finally a decrease in sharpness and resolution of the photographic image. From a microscopic point of view, the solution of the problem is looking for crystals with a large scattering cross section to increase sensitivity and, on the other hand, with a large forward momentum carried by the scattered radiation in order to keep the incident photons parallel.

Since silver halide crystals can be produced oblate up to large axis ratios of 20, optimization of crystal shape in the described sense becomes possible and has been the motivation for this paper. Related theoretical work was already published by *Kurtz* et al. [2] where oblate AgBr particles were modelled by spheroidally shaped particles and the scattering process was calculated by the spheroidal expansion method. *Berdnik* et al. [3] have applied the anomalous diffraction approximation for calculating the radiative transfer equation with orientated spheroidal particles. In this paper the Multiple Multipole Method (MMP) was used to describe the scattering process of an oblate silver halide crystal modelled by a rounded plate with an incident plane wave.

2 MMP-Method

The MMP-method was originally derived by *Hafner* and *Bomholt* [4]. Like all semi-analytical methods

MMP is using analytical solutions to describe the fields of an object or the surrounding medium, whereas a numerical method is applied to solve the boundary value problem. Therefore, there is a large flexibility concerning the particle shape but a restriction to homogeneous volumes.

Two unknown functions, \mathbf{E} and \mathbf{H} , are describing the electric and magnetic field during the scattering process. They have to fulfill the 3-D Helmholtz equation with the wave number k

$$\left(\nabla^2 + k^2\right) \mathbf{U}(\mathbf{r}) = 0 \quad \text{with } \mathbf{U} \in \{\mathbf{E}, \mathbf{H}\} \quad (1)$$

and can be expanded in terms of series of eigenfunctions of Eq. (1) related to *different origins* (that is poles). Because of choosing a spherical coordinate system, the poles include spherical Bessel functions, spherical Hankel functions of the second kind and Legendre functions. To create an over-determined system of algebraic equations which finally is solved by least-squares procedures, the expansions are matched to the boundary conditions at numerous points, the so-called *matching-points*. The number of matching-points rules the over-determination of the system. The boundary conditions include the continuity of the tangential electric and magnetic field components on the bounding surface of the scattering object:

$$\mathbf{n} \times (\mathbf{E}_1 - \mathbf{E}_2) = 0 \quad (2)$$

$$\mathbf{n} \left((\sigma_1 + i\omega\epsilon_1)\mathbf{E}_1 - (\sigma_2 + i\omega\epsilon_2)\mathbf{E}_2 \right) = 0 \quad (3)$$

$$\mathbf{n} \times (\mathbf{H}_1 - \mathbf{H}_2) = 0 \quad (4)$$

$$\mathbf{n}(\mu_1\mathbf{H}_1 - \mu_2\mathbf{H}_2) = 0 \quad (5)$$

\mathbf{n} denotes a normalized vector on a surface element, σ conductivity, ϵ permittivity, and ω the angular frequency. An additional condition which is necessary to guarantee the physical relevance of solutions is the *radiation condition*. It can be regarded as a boundary condition for infinity and limits the asymptotic behaviour of the fields. For 3-D problems it can be written as

$$\lim_{r \rightarrow \infty} r \left[\frac{\partial U(r)}{\partial r} - ik U(r) \right] = 0, \quad (6)$$

where U denotes here any of the field components, r is the radius, and k the wave number. The main problem of this technique is to find the best arrangement of the poles and to choose their order.

3 Light Scattering Simulations

3.1 Description of a Crystal

For all given results the following model of the crystal shape was used. The edges of the crystal do not seem to be important because of its neglectable influence compared to its axis ratio. Therefore, the crystal was modelled by a cylinder with a circumferencing torus like sketched in Fig. 1. The volume of the cylindrical shape on the left side of the figure is given by

$$V_{left} = 2\pi ab^2. \quad (7)$$

The volume of the model pictured on the right can be calculated by integration:

$$V_{right} = \pi \int_{-a}^a \left(b_0 + \sqrt{a^2 - x^2} \right)^2 dx \quad (8)$$

$$= 2\pi ab_0^2 + \frac{4}{3}\pi a^3 + \pi^2 a^2 b_0 \quad (9)$$

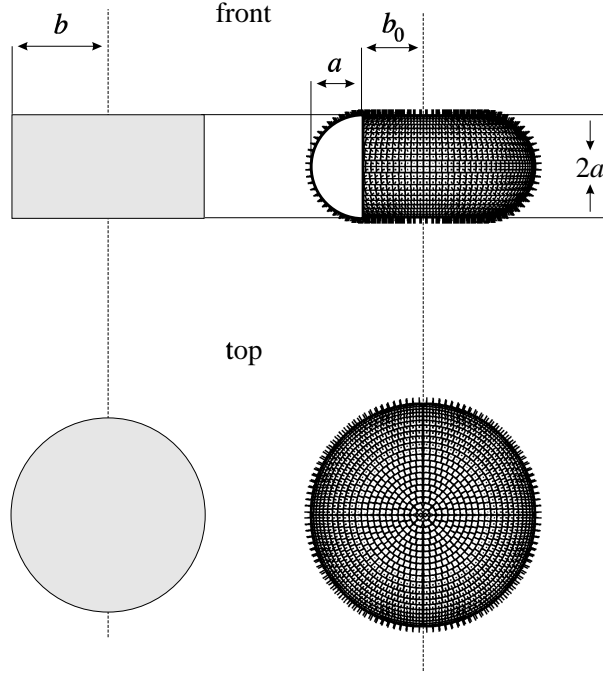


Figure 1: sketch of the model shape

This body is can be built up by a cylinder with the same height, the unknown radius b_0 , and a circumferencing radially cut torus with the small radius a and the large radius b_0 . Both volumes, V_{right} and V_{left} , are defined to be equal. This condition gives the radius b_0 :

$$b_0 = -\frac{\pi}{4}a + \sqrt{a^2 \left(\frac{\pi^2}{16} - \frac{2}{3} \right) + b^2} \quad (10)$$

3.2 General Comparison to a Sphere

All given calculations are given for the following parameters:

- size parameter $x = 15$
- relative refractive index $n_{rel} = 1.5$
- refractive index of embedding gelatine medium $n_{Med} = 1.53$
- axis ratio $b/a = 2$ of the oblate particle
- TE polarization

The size parameter x of an oblate particle is defined by a sphere of equal volume.

$$x = \frac{\pi d_k n_{Med}}{\lambda_0} \quad (11)$$

d_k in this equation denotes the diameter of the sphere with equal volume and λ_0 stands for the vacuum wavelength.

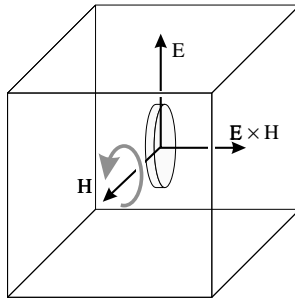


Figure 2: sketch to explain the scattering situation for TE polarization

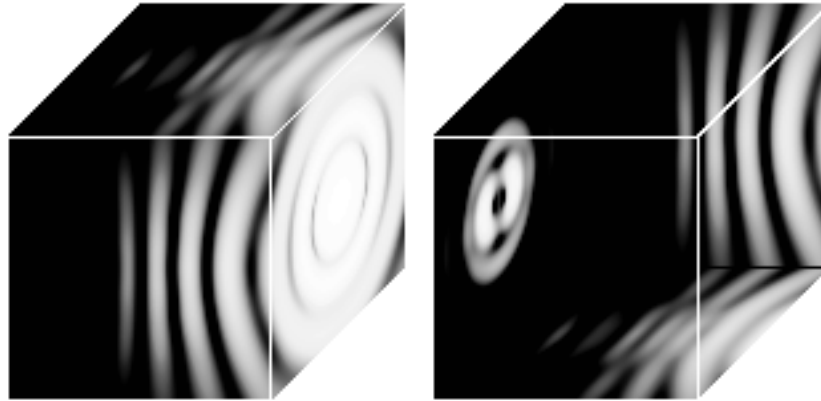


Figure 3: far field intensity of plane wave scattering by a sphere

In order to discuss plane wave scattering of a sphere or a crystal with different orientations a special way of graphical presentation was chosen which will be explained by the sketch in Fig. 2. The scattered intensity is projected onto the surface of a (sufficient large) cube where the colour *white* stands for high intensity. There is a fixed but no linear or other simple color scale, because the scale was chosen in order to maximize contrast. In each case, like in Fig. 3 where the scattered far field intensity of a sphere is given, two cubes are shown. On the left side one can see the visible sides of the cube and on the right the invisible, covered sides. The plane wave is propagating from the left to the right and is vertical polarized in TE case. The orientation of the scattering particle was varied by rotation of the oblate around the magnetic field vector. In the sketch an oblate is pictured with the orientation angle 0° .

As mentioned before, the scattered far field intensity of a sphere can be seen in Fig. 3. On the left cube one can see the forward scattering on its right side. Obviously, the diffractive pattern dominates in forward direction. On the right cube, the back scattering region is given on its left side.

In comparison to this, the far field pattern of the oblate particle in Fig. 4 gives a similar result with a larger number of oscillations in direction of diffraction. This is correct, because the oblate particle with equal volume has a larger diameter than the sphere. The influence of orientation is shown by the following figures 4 to 13 where the oblate particle is rotated around the magnetic field vector by steps of ten degrees.

While forward scattering is dominated by diffraction, one can detect macroscopic effects like reflection

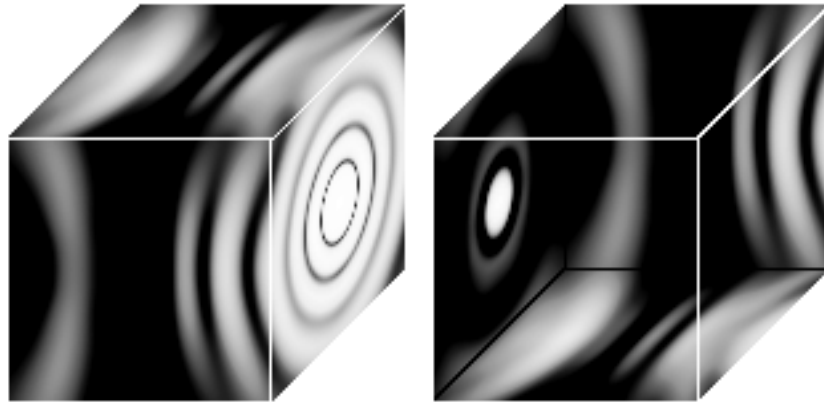


Figure 4: far field intensity of an oblate scatterer with incident angle 0° .

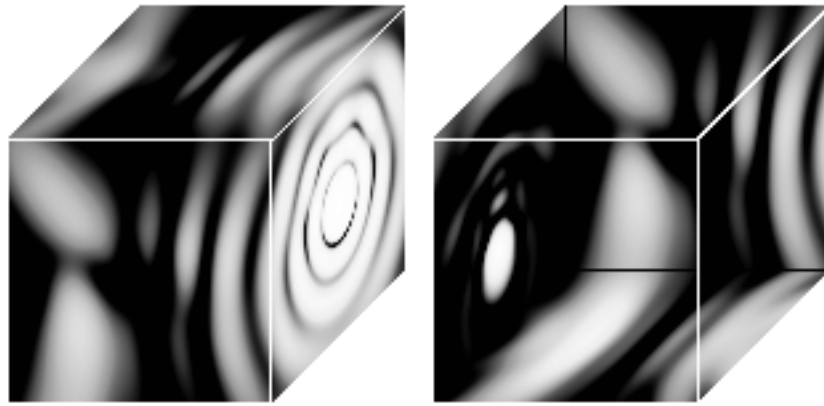


Figure 5: far field intensity of an oblate scatterer with incident angle 10°

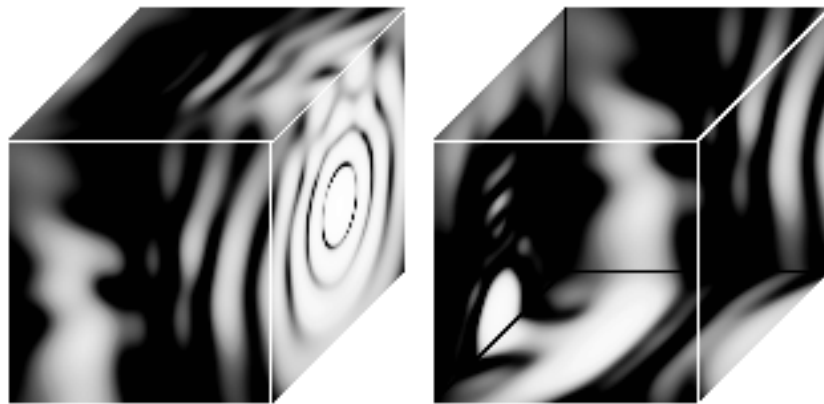


Figure 6: far field intensity of an oblate scatterer with incident angle 20°

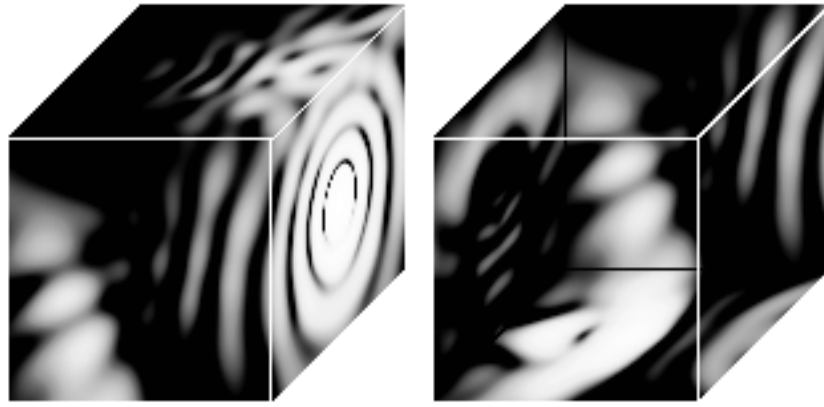


Figure 7: far field intensity of an oblate scatterer with incident angle 30°

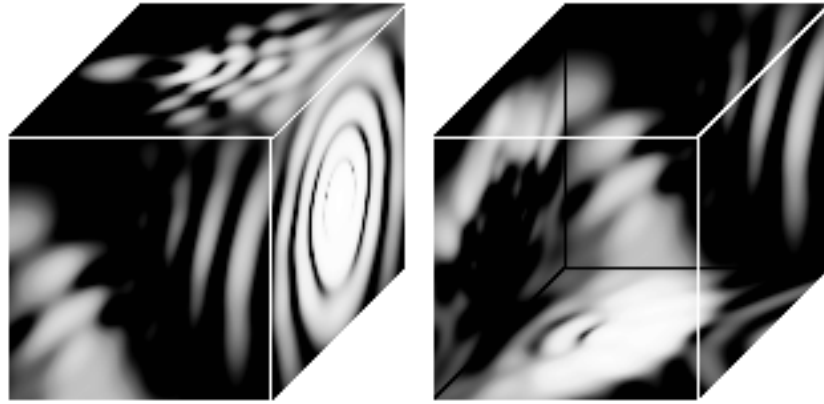


Figure 8: far field intensity of an oblate scatterer with incident angle 40°

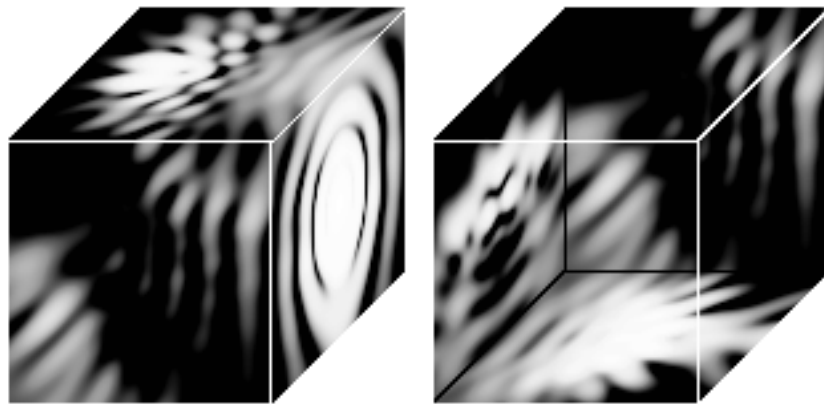


Figure 9: far field intensity of an oblate scatterer with incident angle 50°

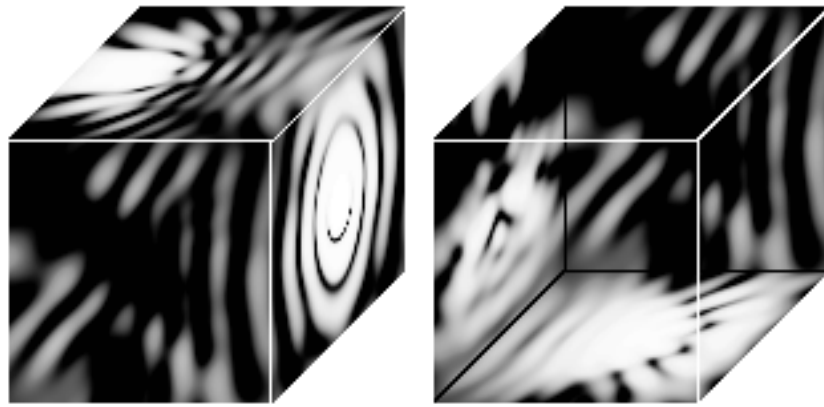


Figure 10: far field intensity of an oblate scatterer with incident angle 60°

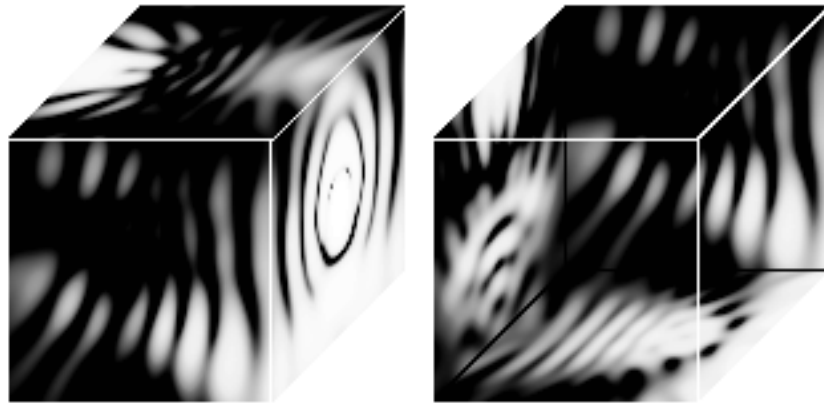


Figure 11: far field intensity of an oblate scatterer with incident angle 70°

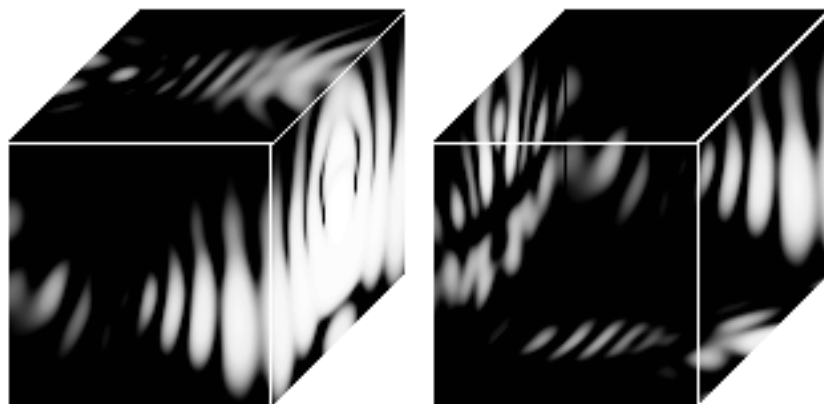


Figure 12: far field intensity of an oblate scatterer with incident angle 80°

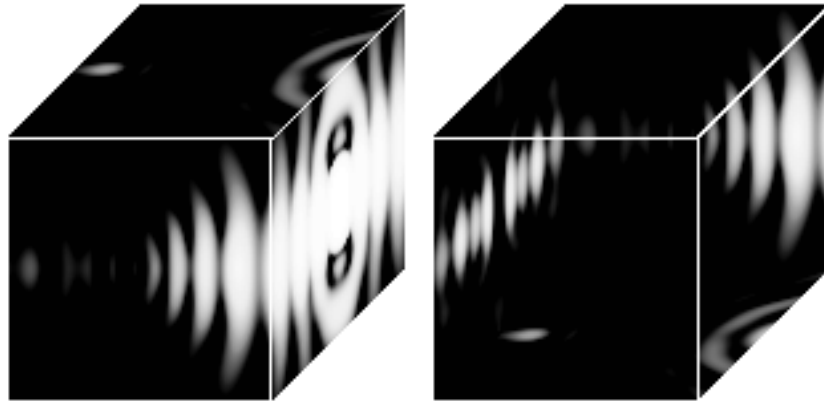


Figure 13: far field intensity of an oblate scatterer with incident angle 90° when the rounded edge of the particle is illuminated

in the back scattering region. The latter can very easily be observed by the movement of the intensity spot on the left side of the right cubes which seems to be reflected onto the flat side of the crystal.

4 Conclusion

The macroscopic behaviour in light scattering of such a small oblate particle underline the large possibilities of optimizing sensitivity and sharpness of a silver halide film by the geometry of its crystals. Even the very small oblate particle with a diameter of a few wavelength shows effects like reflection on its flat side.

5 References

- [1] H.-J. Metz: Zur Berechnung der Streulichtverteilung in photographischen Schichten. PhD thesis. Rheinisch-Westfälische Technische Hochschule Aachen (1968).
- [2] V. Kurtz, S. Salib: Scattering and absorption of electromagnetic radiation by spheroidally shaped particles: Computation of the scattering properties. *Journal of Imaging Science and Technology* 37 (1993), 43–60.
- [3] V. V. Berdnik, V. A. Loiko: Light reflection and transmission by layers with orientated spheroidal particles. *Part. Part. Syst. Charact.* 13 (1996), 171–176.
- [4] C. Hafner, L. Bomholt: *The 3D Electrodynamic Wave Simulator*. John Wiley & Sons Ltd, Chichester (1993).